Supplement of Atmos. Chem. Phys., 19, 15533–15544, 2019
https://doi.org/10.5194/acp-19-15533-2019-supplement


Atmospheric Chemistry and Physics
Open Access
EGU

*Supplement of*

# 21st-century Asian air pollution impacts glacier in northwestern Tibet

**M. Roxana Sierra-Hernández et al.**

*Correspondence to:* M. Roxana Sierra-Hernández (sierra-hernandez.1@osu.edu)

**Table S1.** Limit of detection (LOD), procedural blank (TE concentrations of the water used to make the artificial ice core and of the ice from the artificial ice core), accuracy, and blanks average. LOD corresponds to three times the standard deviation of the concentration of 10 measurements of ultrapure water (18.3 MΩ). The concentrations of the Reference Material (TMRain-95) are reported as total concentrations accounting for the dilution factor of ~20.

| | | Procedural Blank | | Accuracy | |
|---|---|---|---|---|---|
| Trace Element | LOD | Ultrapure water | Artificial ice core | TMRain-95 Found | TMRain-95 Certified |
| Ag (pg $g^{-1}$) | 0.1 | 0.5 ± 0.1 | 1 ± 0.01 | | |
| Al (ng $g^{-1}$) | 0.03 | 0.6 ± 0.6 | 0.9 ± 1.2 | 2 ± 0.9 | 2 ± 0.9 |
| As (pg $g^{-1}$) | 0.8 | 3 ± 0.7 | 4 ± 1 | 1126 ± 153 | 1070 ± 250 |
| Ba (pg $g^{-1}$) | 2 | 27 ± 11 | 32 ± 19 | 762 ± 59 | 730 ± 150 |
| Bi (pg $g^{-1}$) | 0.01 | 0.03 ± 0 | 0.04 ± 0.03 | 802 ± 13 | 630 ± 260 |
| Cd (pg $g^{-1}$) | 0.1 | 0.9 ± 0.5 | 1 ± 0.2 | 468 ± 14 | 480 ± 120 |
| Co (pg $g^{-1}$) | 0.2 | 0.3 ± 0.1 | 1 ± 0.5 | 227 ± 10 | 220 ± 37 |
| Cr (pg $g^{-1}$) | 1 | 3 ± 3 | 7 ± 5 | 770 ± 37 | 790 ± 170 |
| Cs (pg $g^{-1}$) | 0.1 | 1 ± 0.3 | 2 ± 0.5 | | |
| Cu (pg $g^{-1}$) | 1 | 21 ± 4 | 27 ± 5 | 6305 ± 101 | 6200 ± 930 |
| Fe (ng $g^{-1}$) | 0.2 | 0.1 ± 0.2 | 0.4 ± 0.3 | 24 ± 10 | 24 ± 4 |
| Ga (pg $g^{-1}$) | 0.5 | 2 ± 2 | 3 ± 3 | | |
| Li (ng $g^{-1}$) | 0.04 | 0.8 ± 0.3 | 0.7 ± 0.1 | 0.3 ± 0.2 | 0.4 ± 0.08 |
| Mg (ng $g^{-1}$) | 0.02 | 0.2 ± 0.1 | 0.2 ± 0.1 | | |
| Mn (pg $g^{-1}$) | 1 | 4 ± 5 | 5 ± 2 | 6013 ± 77 | 6100 ± 780 |
| Mo (pg $g^{-1}$) | 0.2 | 0.5 ± 0.2 | 1 ± 0.1 | 174 ± 7 | 170 ± 100 |
| Na (ng $g^{-1}$) | 0.4 | 1 ± 0.7 | 2 ± 0.7 | | |
| Nb (pg $g^{-1}$) | 0.2 | 5 ± 2 | 10 ± 6 | | |
| Ni (pg $g^{-1}$) | 0.8 | 3 ± 0.6 | 3 ± 0.8 | 845 ± 35 | 800 ± 170 |
| Pb (pg $g^{-1}$) | 0.3 | 0.43 ± 0.2 | 0.8 ± 0.5 | 281 ± 5 | 290 ± 93 |
| Rb (pg $g^{-1}$) | 1 | 18 ± 18 | 25 ± 16 | | |
| Sb (pg $g^{-1}$) | 0.1 | 0.1 ± 0.03 | 0.1 ± 0.01 | 322 ± 7 | 350 ± 100 |
| Sn (pg $g^{-1}$) | 4 | 2 ± 0.5 | 2 ± 0.7 | | |
| Sr (pg $g^{-1}$) | 5 | 285 ± 133 | 296 ± 132 | 1729 ± 58 | 1700 ± 260 |
| Ti (pg $g^{-1}$) | 10 | 21 ± 26 | 31 ± 24 | | |
| Tl (pg $g^{-1}$) | 0.02 | 0.03 ± 0.01 | 0.05 ± 0.02 | 330 ± 6 | 330 ± 72 |
| U (pg $g^{-1}$) | 0.03 | 0.07 ± 0.01 | 0.09 ± 0.02 | 262 ± 5 | 250 ± 60 |
| V (pg $g^{-1}$) | 1 | 4 ± 4 | 7 ± 5 | 678 ± 39 | 640 ± 120 |
| Zn (pg $g^{-1}$) | 3 | 8 ± 4 | 5 ± 1 | | |

**Table S2.** Loadings and communalities of each Trace Element (TE) of the first three factors for the entire concentration data set (1971–2015).

| TE | Factor 1 | Factor 2 | Factor 3 | Communality |
|---|---|---|---|---|
| Ag | 0.92 | -0.29 | 0.16 | 0.95 |
| Al | 0.96 | -0.24 | 0.07 | 0.99 |
| As | 0.83 | -0.50 | 0.02 | 0.94 |
| Ba | 0.85 | -0.47 | 0.07 | 0.96 |
| Bi | 0.94 | -0.25 | 0.15 | 0.97 |
| Cd | 0.79 | -0.30 | 0.50 | 0.97 |
| Co | 0.96 | -0.26 | 0.08 | 0.99 |
| Cr | 0.96 | -0.26 | 0.08 | 0.99 |
| Cs | 0.95 | -0.25 | -0.02 | 0.97 |
| Cu | 0.93 | -0.32 | 0.10 | 0.98 |
| Fe | 0.96 | -0.25 | 0.06 | 0.99 |
| Ga | 0.96 | -0.26 | 0.06 | 0.99 |
| Li | 0.79 | -0.56 | 0.01 | 0.95 |
| Mg | 0.80 | -0.57 | 0.05 | 0.96 |
| Mn | 0.84 | -0.43 | 0.18 | 0.92 |
| Mo | 0.41 | -0.85 | 0.08 | 0.90 |
| Na | 0.09 | -0.96 | 0.03 | 0.93 |
| Nb | 0.94 | -0.28 | -0.02 | 0.96 |
| Ni | 0.95 | -0.28 | 0.10 | 0.99 |
| Pb | 0.93 | -0.24 | 0.24 | 0.97 |
| Rb | 0.94 | -0.32 | -0.01 | 0.99 |
| Sb | 0.78 | -0.57 | 0.04 | 0.93 |
| Sn | 0.82 | -0.36 | 0.30 | 0.89 |
| Sr | 0.20 | -0.95 | 0.07 | 0.94 |
| Ti | 0.79 | -0.58 | 0.04 | 0.96 |
| Tl | 0.92 | -0.35 | 0.11 | 0.98 |
| U | 0.82 | -0.50 | 0.08 | 0.93 |
| V | 0.95 | -0.29 | 0.07 | 0.99 |
| Zn | 0.94 | -0.24 | 0.21 | 0.99 |
| Variance (%) | 72.6 | 21.4 | 2.1 | |
| Cum. Variance (%) | 72.6 | 94.0 | 96.1 | |

**Guliya's 1650–2015 trace element records**

In Thompson et al. (2018), we showed the high reproducibility between the 1992 and 2015 Guliya $\delta^{18}O$ profiles. This reproducibility is also observed in the TE records (Figure S1). Likewise, the Al and Fe concentrations show good agreement during the 1971–1991 period in which both TE records overlap (Fig. S1) with median concentrations of 0.3 µg $g^{-1}$ in both records.

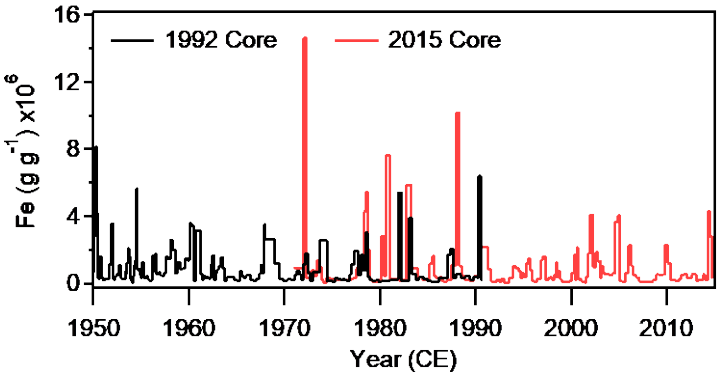


**Figure S1**. Comparison of Fe concentrations at full resolution in the 1992 and the 2015 Guliya ice cores.

Figure S2 displays 5-year median concentrations and EFs of the 1992 (1650–1991) and 2015 (1971–2015) cores for TEs that showed post-1850s enrichments (Pb, Cd, Zn, and Al for comparison). The 5-year median concentrations of Cd, Pb, and Zn are slightly higher in the 2015 record than the 1992 time series for the 1971–1991 period. For example, the Cd median concentrations are 5 and 6 pg $g^{-1}$ in the 1992 and 2015 records, respectively. The difference in concentrations between the 1992 and the 2015 records is not significant (Mann–Whitney test: $p < 0.0005$ for medians) and may be due to spatial variability of ice layers between the two boreholes. Similarly, during the 1971–1991 period, the EFs in the 2015 record are slightly higher than in the 1992 record. This might result from the natural signal to noise ratio differences between the two records. Despite the slight EF differences between the two records during the 1971–1991 period, the reproducibility of TEs allows determination of temporal trends from pre-industrial times (~1650) into the 21st century (2015) using the 1992 and the 2015 TE records.

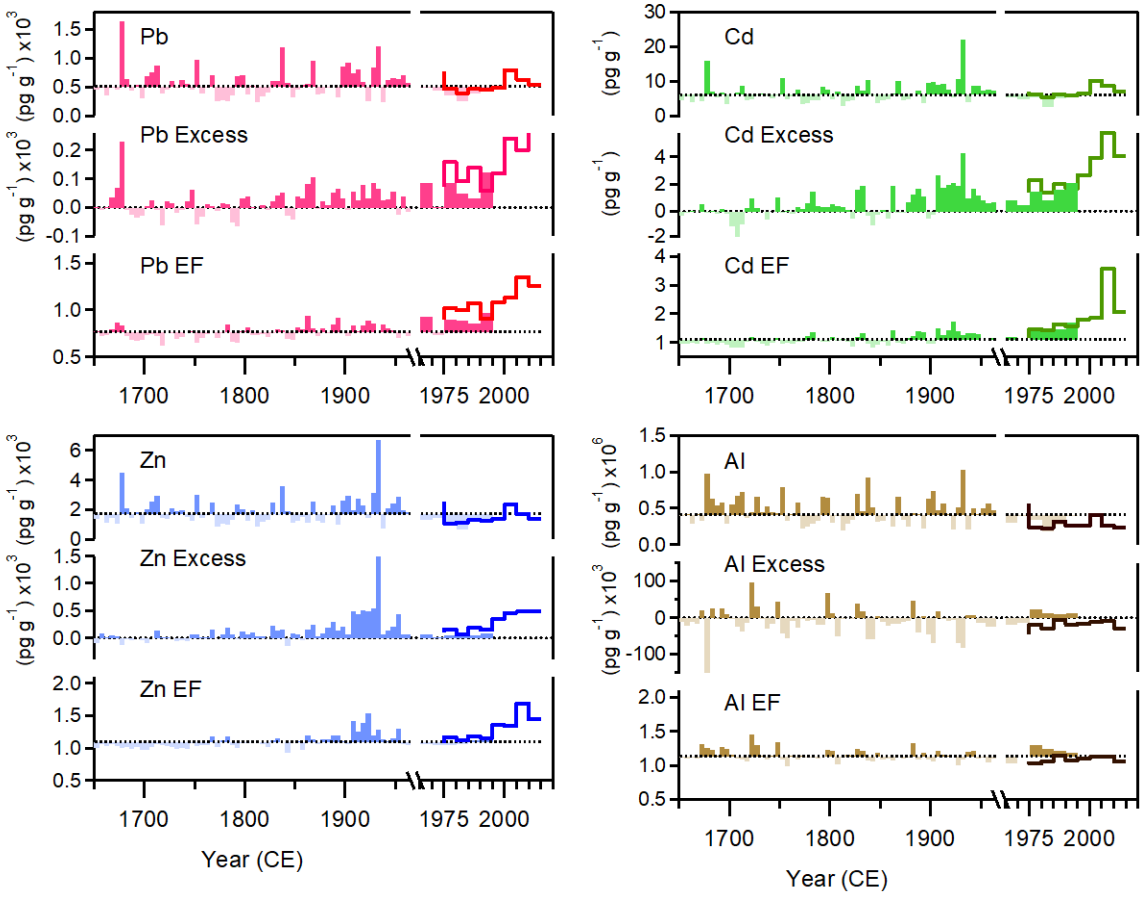


78

79 **Figure S2.** Pb, Cd, Zn, and Al shown as 5-year median concentrations, excess concentrations and enrichment factors
80 (EF) from the 1992 Guliya ice core (1650–1991) and the 2015 Guliya ice core (1971–2015; thick line). The
81 horizontal dotted lines show the 1650–1991 concentration and EF medians for the 1992 core.

82

83

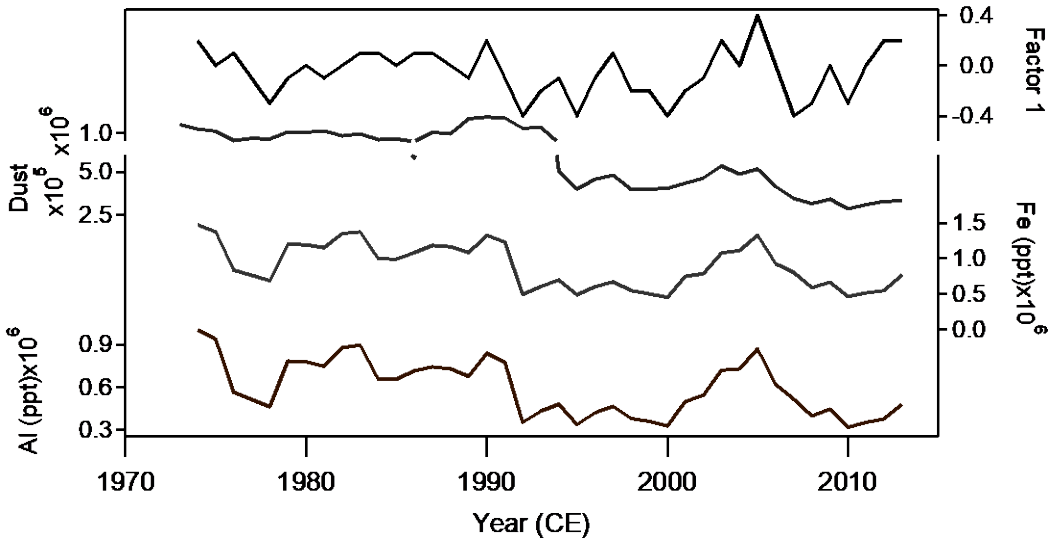


**Figure S3.** Comparison of Factor 1 scores (crustal contribution), dust concentrations (particles $ml^{-1}$) (Thompson et al., 2018), and concentrations of the typical crustal TEs Fe and Al. All data are presented as five-year running means.

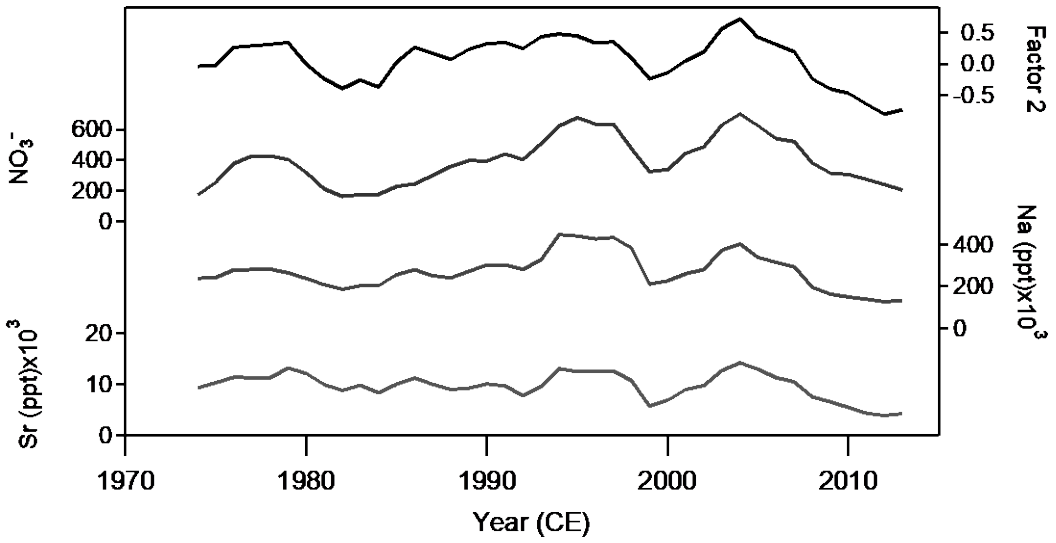


**Figure S4.** Comparison of Factor 2 scores (evaporitic contribution), $NO_3^-$ ion concentrations (Thompson et al., 2018), and TEs concentrations of sodium (Na) and strontium (Sr). All data are presented as five-year running means.

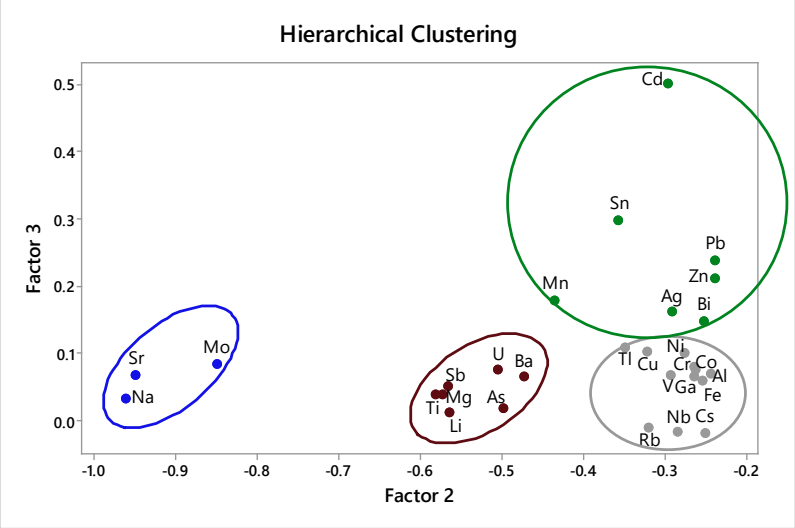


93

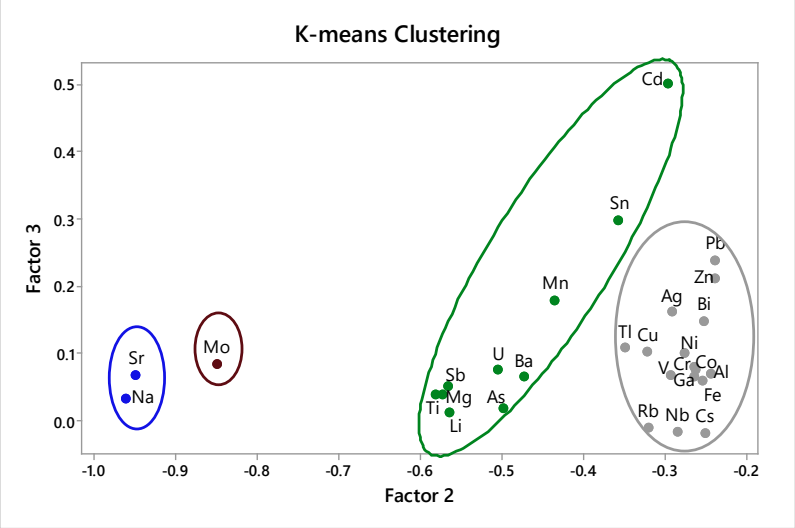


94

95 **Figure S5**. Hierarchical and non-hierarchical (K-means) cluster analysis extracted from the first three factors during
96 the 1971–2015 period.

97

98

99

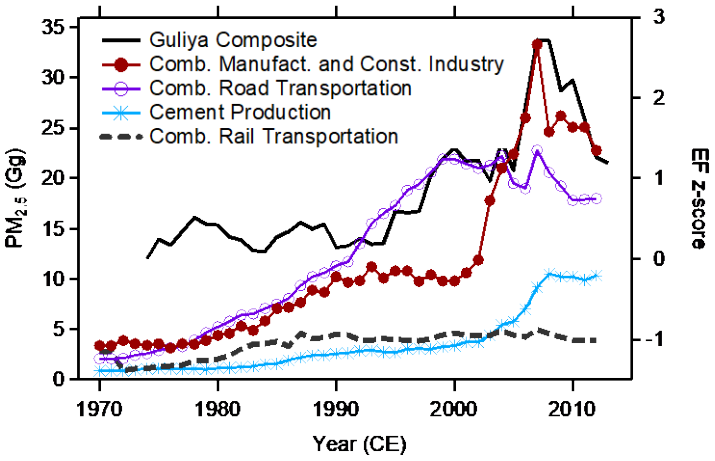


**Figure S6**. Largest emitter sectors of $PM_{2.5}$ in Pakistan between 1970 and 2012: fossil fuel combustion in manufacturing and construction industries, fossil fuel combustion by road transportation, cement production, and fossil fuel combustion by rail transportation (EDGARv4.3.2, 2017; Crippa et al., 2018). The Guliya EF composite (average of Cd, Pb, Zn, and Ni EF z-scores) is shown for comparison.

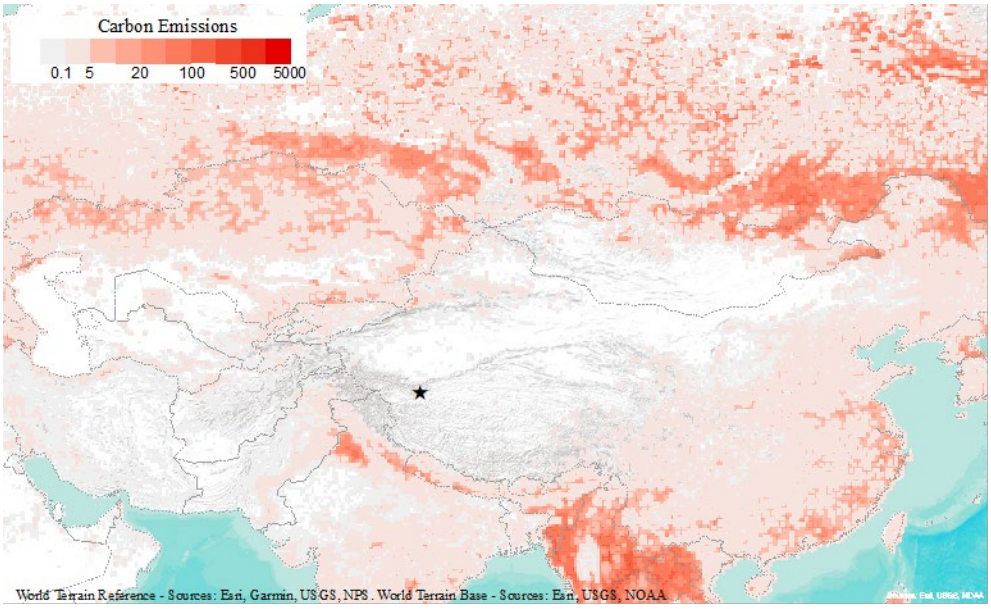


**Figure S7**. Annual carbon emissions (g C $m^{-2}$ $year^{-1}$) from fires averaged over the 1997–2016 period (van der Werf et al., 2017). The Guliya ice cap location is indicated in the map with a star.

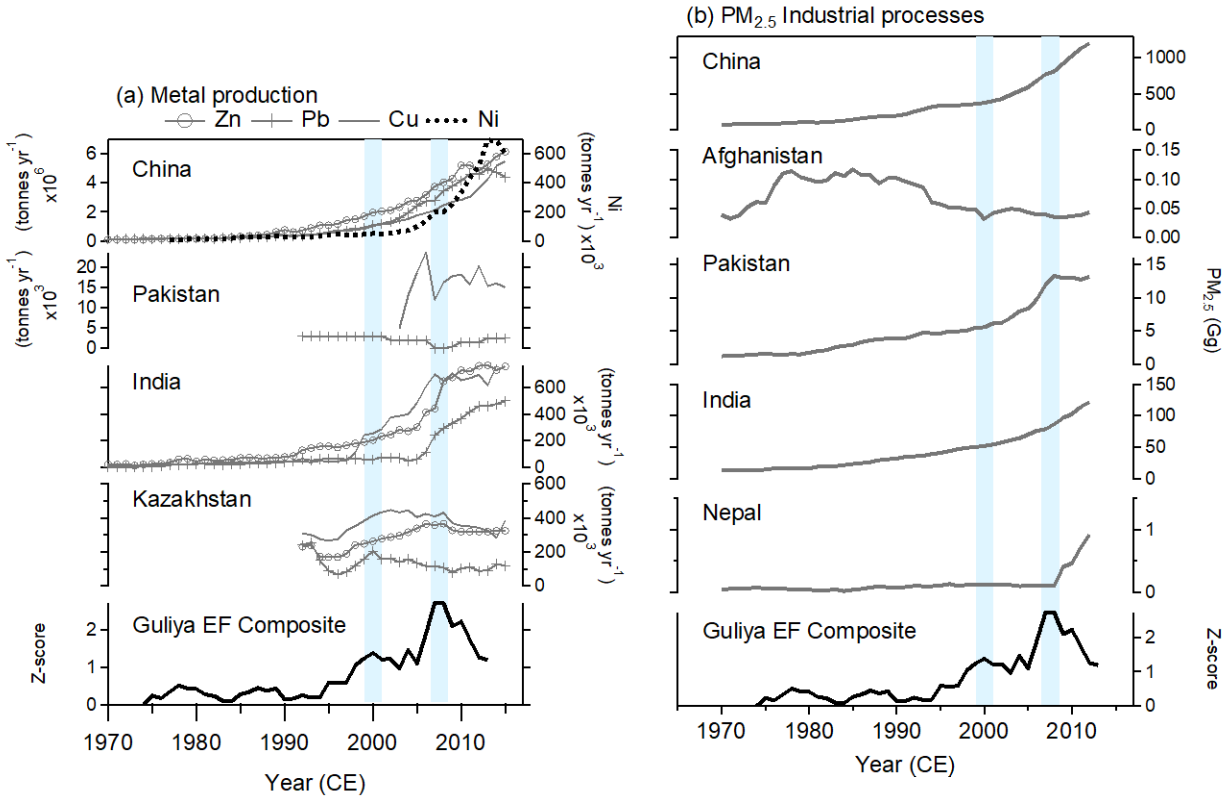


**Figure S8**. (a) Metal production in China (Zn, Pb, Cu, and Ni), Pakistan (Pb, Cu), India (Zn, Pb, Cu) and Kazakhstan (Zn, Pb, Cu) (BGS, 2015) and (b) $PM_{2.5}$ from industrial processes (including the production of cement, lime, chemicals, and metal production). The Guliya EF composite (average of Cd, Pb, Zn, and Ni EF z-scores) is shown at the bottom of each panel for comparison. The two Guliya maxima at 2000 and 2008 are shown as shaded bars.

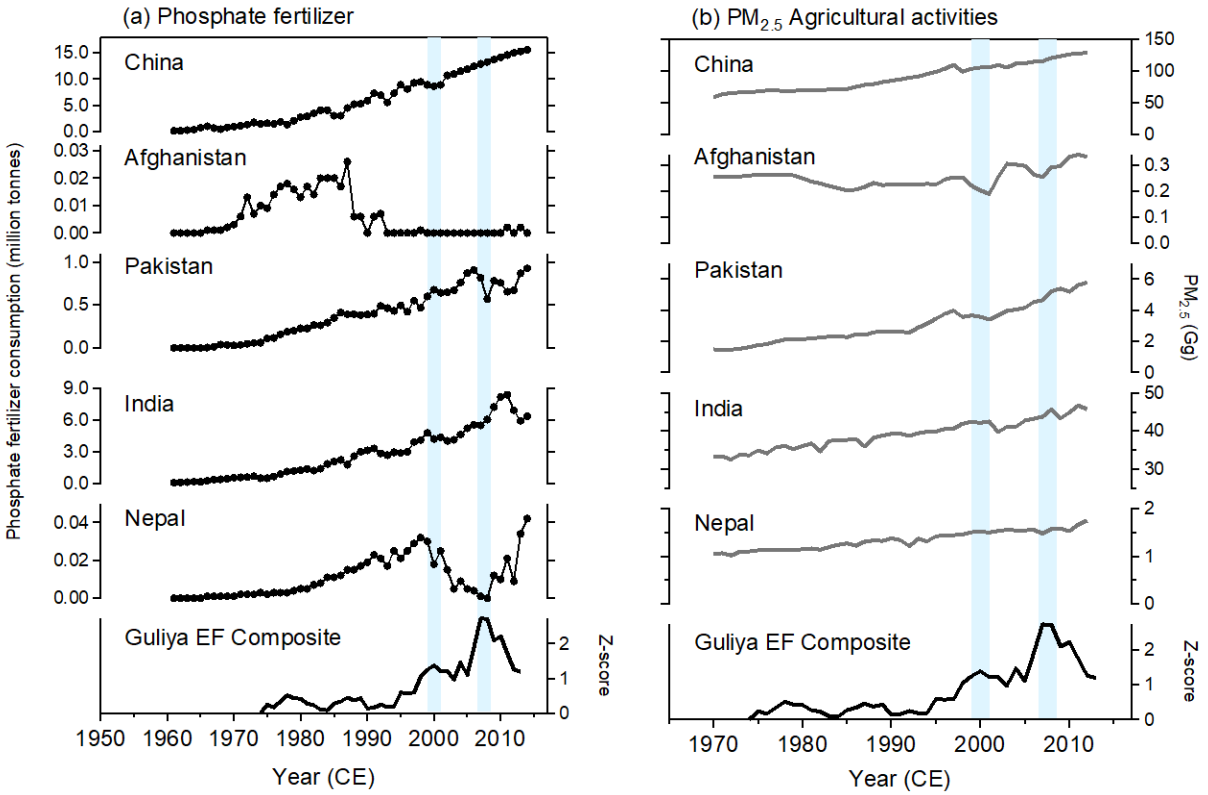


**Figure S9.** (a) Phosphate fertilizer consumption (FAO, 2019) and (b) $PM_{2.5}$ from agricultural activities (including direct soil emission, rice cultivation, and manure management) (EDGARv4.3.2, 2017; Crippa et al., 2018). The Guliya EF composite (average of Cd, Pb, Zn, and Ni EF z-scores) is shown at the bottom of each panel for comparison. The two Guliya maxima at 2000 and 2008 are shown as shaded bars.

## References


BGS, British Geological Survey. World Mineral Statistics and World Mineral Production, 2/1/2018, 2015.

Crippa, M., D. Guizzardi, M. Muntean, E. Schaaf, F. Dentener, J. A. van Aardenne, S. Monni, U. Doering, J. G. J. Olivier, V. Pagliari and G. Janssens-Maenhout, Gridded emissions of air pollutants for the period 1970–2012 within EDGAR v4.3.2. Earth Syst. Sci. Data, 10, 1987-2013, 10.5194/essd-10-1987-2018, 2018.

EDGARv4.3.2, European Commission, Joint Research Centre (EC-JRC)/Netherlands Environmental Assessment Agency (PBL). Emissions Database for Global Atmospheric Research (EDGAR), release EDGAR v4.3.2 (1970 - 2012), 2017.

FAO, Food and Agricultural Organization of the United Nations . Phosphate Fertilizer Consumption, 4/22/2019, 2019.

Thompson, L. G., T. Yao, M. E. Davis, E. Mosley-Thompson, G. Wu, S. E. Porter, B. Xu, P.-N. Lin, N. Wang, E. Beaudon, K. Duan, M. R. Sierra-Hernández and D. V. Kenny, Ice core records of climate variability on the Third Pole with emphasis on the Guliya ice cap, western Kunlun Mountains. Quat. Sci. Rev., 188, 1-14, 2018.

van der Werf, G. R., J. T. Randerson, L. Giglio, T. T. van Leeuwen, Y. Chen, B. M. Rogers, M. Mu, M. J. E. van Marle, D. C. Morton, G. J. Collatz, R. J. Yokelson and P. S. Kasibhatla, Global fire emissions estimates during 1997–2016. Earth Syst. Sci. Data, 9, 697-720, 10.5194/essd-9-697-2017, 2017.